Morphological Studies of Binary Mixtures of Block Copolymers. 2. Chain Organization of Long and Short Blocks in Lamellar Microdomains and Its Effect on Domain Size and Stability

François Court[†,‡,§] and Takeji Hashimoto[*,†]

Department of Polymer Chemistry, Graduate School of Engineering, Kyoto University, Kyoto 606-8501, Japan, and Laboratoire de Physico-Chimie Structurale et Macromoléculaire, ESPCI, 10 rue Vauquelin, 75005 Paris, France

Received September 7, 2001; Revised Manuscript Received December 11, 2001

ABSTRACT: We focus on chain organization of long and short block chains on lamellar microdomains developed in a series of binary mixtures denoted as as/s_i, which are composed of a long asymmetric polystyrene-*block*-polyisoprene (SI) and one of three short symmetric SI's denoted respectively as *as* and s_i ($i = 1, 2, 3$). We investigated the effect of chain organization on stability of the microdomain and on microdomain size as a function of blending composition and ratio of degree of polymerization of *as* to s_i. Comparisons of the results with some theoretical predictions indicated that the strong segregation theory of Birshtein, Zhulina, and Lyatskaya fits well with the experimental results.

I. Introduction

In a previous paper,[1] we explored morphological behavior of a series of three kinds of binary mixtures of polystyrene-*block*-polyisoprene diblock copolymer (SI) composed of a long asymmetric SI denoted as *as* with degree of polymerization (DP) denoted as N_{as} and a short symmetric SI denoted as s_i ($i = 1$, 2, or 3) with DP denoted as N_{si} ($i = 1$, 2, or 3). All the blends studied were miscible at the molecular level, yielding a single ordered morphology or a disordered single phase. A phase diagram of such blends as/s_i ($i = 1$, 2, or 3) was investigated in the parameter space of the ratio $r \equiv N_{as}/N_{si}$ and overall volume fraction of PS block ϕ_{PS}, the latter of which depends on blending composition of the mixtures as/s_1, as/s_2, and as/s_3. Although the morphology encountered by changing composition of block copolymers are the common ones found in neat SI, such as spheres in a body-centered-cubic lattice, hexagonal cylinders, bicontinuous structures, and lamellae, the stability limit of each morphology is significantly shifted with respect to ϕ_{PS}, which is a unique point found in the previous study. More uniquely, the shift increases with increasing the ratio *r*. As a consequence, mixing of a small amount of the symmetric blocks s_i ($i = 1$, 2, or 3) into the majority component of asymmetric blocks *as* effectively changes the interface curvature and hence enlarges very much the composition range where the lamellar microdomains are developed. This so-called *cosurfactant effect* was found to become more remarkable as the molecular weight ratio proportional to *r* gets bigger.

In this paper we focus our attention on how block copolymers with two different chain lengths are organized in a common microdomain space with their junction localized at common interfaces to give the intriguing cosurfactant effect and aim to explore how the chain organization of different block lengths affects the microdomain size as well as the stability limit of the microdomains. Studying the lamellar morphology presents the following advantages. Lamellae tend to be very well organized with a long-range order. Therefore, their SAXS signature is characterized by a numerous well-defined scattering maxima, which enables us to evaluate the lamellar spacing very accurately from each of those diffraction maxima. Furthermore, the symmetry of the lamellar morphology is very simple, allowing a direct determination of Σ, the interfacial area per junction. It should be noted that we have been acutely aware of the previous studies, which have an attempt similar to this study. For example, Hadziioannou and Skoulios had investigated the domain spacing and morphologies of the binary blends of SI block copolymers as early as 1982.[2] Later on, Vilesov et al.,[3] Spontak and co-workers,[4,5] and Lin et al.[6] had done excellent works concerning the relation between the domain spacing of lamellar microdomain and the chain organization of different block lengths in their own binary blends of diblock copolymer systems. Nevertheless, we believe that this study is rich enough in new aspects including comprehensive comparisons of previous works.

II. Experimental Methods

II.1. Samples. SI diblock copolymers were prepared by sequential living anionic polymerization following the method described in the previous publication.[1] For each synthesis a sample was taken before adding isoprene monomers to measure the molecular weight of the first polymerized polystyrene block by size exclusion chromatography. Table 1 summarizes the characteristics of the different diblocks synthesized.

II.2. Film Specimens. The film specimens of neat SI diblocks (*as*, s_i) and their binary mixtures (as/s_1, as/s_2, and as/s_3) were prepared in the same way. 10 wt % polymer solutions were obtained by dissolving the polymer(s) with toluene as a neutrally good solvent for both PS and PI. The solution which was homogeneous and disordered was stirred for 5 h and then placed in a Petri dish in a controlled atmosphere at 25 °C. The slow evaporation process of the solvent lasted over 3 weeks. The film specimens were further dried at 80 °C under vacuum until constant weights were attained. The thickness of the cast films was ca. 400 μm.

II.3. Small-Angle X-ray Scattering. The microdomain structures were investigated by small-angle X-ray scattering

† Kyoto University.
‡ ESPCI.
§ Present address: Centre d'Etude de Recherche et de Développement d'ATOFINA, 27470 Serquigny, France.
* To whom correspondence should be addressed.

10.1021/ma011588c CCC: $22.00
Published on Web 02/28/2002

Table 1. Characteristics of the SI Diblocks $\bar{M}_n$

diblock codes	$\bar{M}_n \times 10^{-3}$ [a]	HI[b]	$\bar{M}_{n,PS} - \bar{M}_{n,PI} \times 10^{-3}$ [c]	$N_{PS} - N_{PI}$[d]	N[e]	w_{PS}[f]	f_{PS}[g]
as	47.0	1.03	9.6−37.4	92−550	642	0.205	0.185
s_1	18.6	1.03	9.6−9.0	92−132	224	0.515	0.485
s_2	14.5	1.03	7.0−7.5	67−110	177	0.485	0.455
s_3	12.1	1.03	6.3−5.8	61−85	146	0.52	0.49

[a] $\bar{M}_n$: number-average molecular weight determined by size exclusion chromatography (SEC). [b] HI = $\bar{M}_w/\bar{M}_n$: heterogeneity index for molecular weight distribution. [c] $\bar{M}_{n,k}$: number-average molecular weight of the kth block (k = PS or PI). [d] N_k: number-average degree of polymerization of the kth block (k = PS or PI). [e] N: total number-average degree of polymerization of the diblock: $N = N_{PS} + N_{PI}$. [f] w_{PS}: polystyrene weight fraction in SI block copolymer. [g] f_{PS}: volume fraction of the PS block calculated from $f_{PS} = (w_{PS}/\rho_{PS})/(w_{PS}/\rho_{PS} + (1 - w_{PS})/\rho_{PI})$ by using the following densities for the PS and PI blocks, $\rho_{PS} = 1.0514$ g cm^{-3} and $\rho_{PI} = 0.925$ g cm^{-3}.

(SAXS) using a Rigaku rotating anode X-ray generator operated at 50 kV and 200 mA.[7−9] The X-ray is monochromated with a graphite crystal, and its wavelength λ is 0.154 nm (Cu Kα line). The scattered intensity is measured with a one-dimensional position sensitive proportional counter with the sample-to-camera distance of 1166 mm. The SAXS profiles were corrected for the air scattering, the absorption, the slit height, and slit width smearing effects.[7−10] The absolute SAXS intensity was determined by the Nickel foil method.[11] Each profile was recorded at room temperature over a period of 2 h. The profiles are represented as a function of magnitude of scattering vector **q**, q, which is related to the scattering angle, θ, by eq 1:

$$q = (4\pi/\lambda)\sin(\theta/2) \quad (1)$$

The scattered intensity is represented on a logarithmic scale in arbitrary units.

II.4. Determination of the Lamellar Spacing, *D*. The SAXS profile of a sample with a well-ordered lamellar morphology presents several diffraction maxima. The position of the ith diffraction maxima, q_{mi}, is related through eq 2 to the periodicity of the morphology, D, a sum of the thickness of the PS and the PI lamellae:

$$D = 2\pi i/q_{mi} \quad (i = 1, 2, ...) \quad (2)$$

For each sample, the determination of D was done using eq 2 applied to the different order (i) of Bragg diffractions observed (at least three) on the SAXS profile. The discrepancy between the values of D obtained on a given sample never exceeded ±0.15 nm.

II.5. Determination of the Interfacial Area per Junction, Σ. In the strong segregation regime, the thickness of the interphase between the different microdomains of an A−B diblock copolymer is negligible compared with D. This zone separating the two blocks A and B can be considered as an interface. The AB blocks form A and B brushes "grafted" or anchored on each side of this interface. This double brush can be characterized by the average interfacial area Σ occupied per a single junction of A−B block. We have investigated this parameter Σ as a function of the blend composition and molecular weight ratio r. First, we will recall the expression of Σ in the case of a pure A−B diblock and then generalize this expression to the case of a blend of two diblocks $(A-B)_\alpha/(A-B)_\beta$ (noted *as* and s_i (i = 1, 2, or 3) in this study).

(a) Pure Diblock. Let us first consider the case of a pure diblock. On the basis of Helfand's theory,[12−15] Hadziioannou and Skoulios[16] proposed that the two brushes forming a lamella are not interpenetrated in the direction normal to the interface. Other works corroborate this point.[17,18] Therefore, the height of the double brush, H_0, can be assumed to be equal to half the period of the lamellae, $D_0/2$. The organization of the diblock chains within the lamellae can be schematically represented in Figure 1. The average volume, V, occupied by one chain is defined by eq 3.

$$V = \Sigma_0 H_0 = \Sigma_0 D_0/2 \quad (3)$$

Under the assumption that the material is incompressible, the volume occupied by one chain is the volume of one monomer times the number of monomers in the chain, i.e., degree of polymerization (DP). Hence, the expression becomes

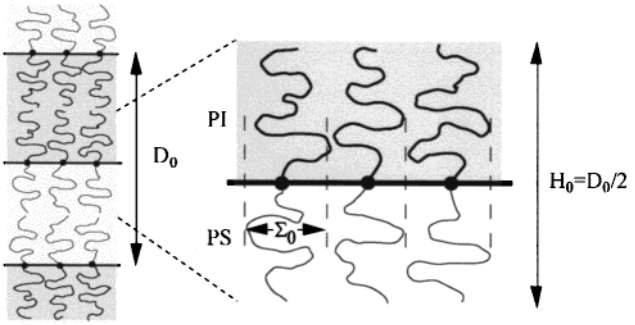

Figure 1. Schematic representation of the organization of the chains of a pure symmetric diblock in a lamellar morphology. D_0 is the lamellae thickness, and Σ_0 corresponds to the average interfacial area per junction.

$$V = N_{PS}v_S + N_{PI}v_I \quad (4)$$

where N_{PS} and N_{PI} are respectively DP of the PS and PI blocks of the diblock, and v_S and v_I are the volume of a styrene and an isoprene monomer unit, respectively. v_i (i = S or I) is given by eq 5.

$$v_i = M_i/(\rho_i N_A) \quad (5)$$

where ρ_i is the mass density of ith polymer, M_i is the molar mass of monomer i, and N_A is Avogadro's number. With $\rho_S = 1.0514$ g cm^{-3}, $\rho_I = 0.925$ g cm^{-3}, $M_S = 104$ g mol^{-1}, $M_I = 68$ g mol^{-1}, and $N_A = 6.023 \times 10^{23}$ mol^{-1}, one gets $v_S = 0.164$ nm^3 and $v_I = 0.122$ nm^3.

Using eqs 2 and 3, the interfacial area per junction, Σ_0, can be expressed as a function of the lamellar period, D_0, and of the molecular characteristics of the monomers constituting the diblocks:

$$\Sigma_0 = 2(N_{PS}v_S + N_{PI}v_I)/D_0 \quad (6)$$

(b) Binary Mixture of Diblocks. Let us focus on the case of our interest, the binary mixture of two SI diblocks *as* and s_i (i = 1, 2, or 3). To express the average interfacial area per junction in the blend, Σ, an assumption must be made: we have to assume first that the system is strongly segregated, the PS blocks and the PI blocks of both *as* and s_i segregate into their own domains without intermixing of different blocks, and second that the two diblocks *as* and s_i (i = 1, 2, or 3) are miscible at a molecular level with their junctions of each diblock, *as* and s_i, segregating on the same interface. The morphological investigation of the series of blends *as*/s_1, *as*/s_2, and *as*/s_3 presented in the previous paper indicates that this assumption is legitimate. Then Σ can be expressed as a function of the composition of the blend *as*/s_i, in terms of the number fraction of long chains *as*, n_{as}:

$$\Sigma = 2\{[(1 - n_{as})N_{si,PS} + n_{as}N_{as,PS}]v_S + [(1 - n_{as})N_{si,PI} + n_{as}N_{as,PI}]v_I\}/D \quad (7)$$

or

$$\Sigma = 2\{N_{si,PS}\nu_S[1 + n_{as}(N_{as,PS}/N_{si,PS} - 1)] + N_{si,PI}\nu_I[1 + n_{as}(N_{as,PI}/N_{si,PI} - 1)]\}/D \quad (8)$$

where $N_{si,PS}$ and $N_{si,PI}$ are the DP's of the PS and PI blocks of the diblocks s_i (i = 1, 2, or 3) and $N_{as,PS}$ and $N_{as,PI}$ are those of the diblock *as*, respectively. For a blend *as*/s_i of a given composition all the terms in eq 8 are known, except D, which is measured experimentally by SAXS analysis. Note here that n_{as} is defined by

$$n_{as} = (w_{as}/\bar{M}_{n,as})/[w_{as}/\bar{M}_{n,as} + (1 - w_{as})/\bar{M}_{n,si}] \quad (9)$$

where w_{as} is weight fraction of the diblock *as* in the blend, and $M_{n,as}$ and $M_{n,si}$ are number-average molecular weights of *as* and s_i (i = 1, 2, or 3), respectively.

III. Results

III.1. *as*/s_1 Mixtures. A series of the blends of *as* and s_1 have been prepared as described previously. s_1 has a lamellar morphology, but *as* has a microdomain structure of PS spheres in a PI matrix. The addition of *as* diblock to s_1 does not induce morphological change, and hence the lamellar structure is maintained as long as w_{as} remains smaller than 0.59 (which corresponds to a chain fraction n_{as} of *as* diblocks of 0.365 as shown in Figure 2). Three blends were investigated within this composition range. Their SAXS profiles are presented in Figure 2 together with the SAXS profiles of neat s_1 and *as*. It is clear in Figure 2 that the position of each Bragg reflection shifts toward smaller q with increasing the fraction of long asymmetric chains in the mixture. The period D of each sample has been determined as described previously, and the results are summarized in Table 2. Using this measured value D and the DP's of the different blocks (Table 1), eq 7 (or eq 8) enabled us to calculate the average interfacial area per junction for each system, Σ. The results obtained are also summarized in Table 2. Figure 3 presents the values D and Σ as a function of the blend composition n_{as}. It is fascinating to observe that the interfacial area per junction is hardly modified when long asymmetric chains are incorporated within the lamellae: D increases but Σ remains constant and equal to Σ_0 (interfacial area per junction in the pure short symmetric diblock).

III.2. *as*/s_2 Mixtures. The symmetric diblock s_2 has a slightly lower molecular weight than s_1. It was found[1] that this reduction of molecular weight extends the stability range of the lamellar morphology toward a smaller volume fraction of PS, Φ_{PS}, or a large volume fraction of *as*. Up to w_{as} of 0.68 (or down to Φ_{PS} = 0.268), the morphology of the blend *as*/s_2 remained lamella. The SAXS profiles of several blends are presented in Figure 4. The period D determined experimentally and the interfacial area per junction Σ calculated for each system are summarized in Table 3. Figure 5 shows the values of D and Σ as a function of n_{as}. As in the first series *as*/s_1, we observe that for the *as*/s_2 series as well the lamellar spacing increases significantly when the fraction n_{as} of *as* chains in the blend increases, but Σ is unaffected with n_{as}.

In the two series of blends investigated, upon adding the long asymmetric diblock *as* to the short symmetric ones s_1 or s_2, one can increase the lamellar thickness by up to 60% and 90%, respectively. However, over the whole composition range investigated, the variations of Σ do not exceed ±2.5%. The average interfacial area per junction in the blends remains equal to the average interfacial area per junction in the pure symmetric diblock, $\Sigma = \Sigma_0$. Consequently, the short symmetric diblock seems to control the interfacial area per junction; the long asymmetric diblock has to fit in the brushes composed of s_1 or s_2 so that a part of the *as* chain in the

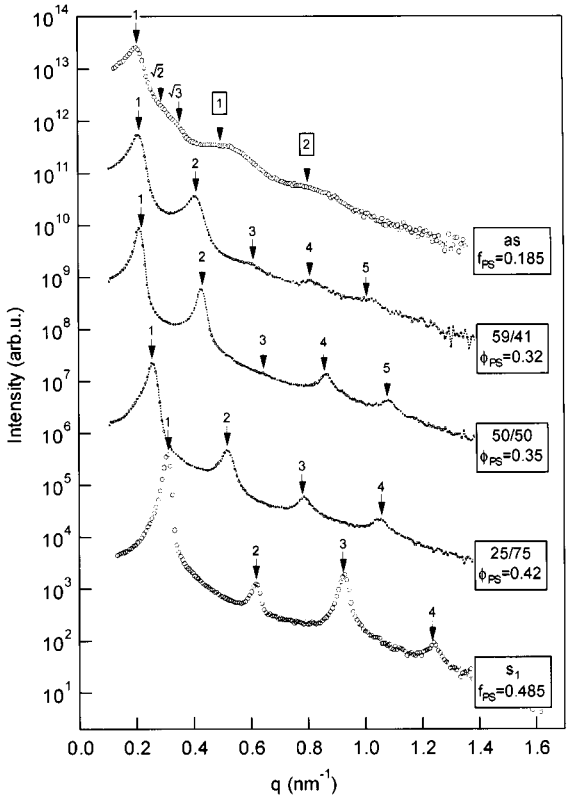

Figure 2. SAXS profiles of *as*/s_1 mixtures with various blend compositions. The composition of the blend, expressed in weight percent of *as* and s_1 in the form of *as*/s_1, is indicated on the profiles. Φ_{PS} designates the total volume fraction of the PS block in the blend.

Table 2. Characteristics of the Blends of the *as*/s_1 Series Presenting a Lamellar Morphology

blend	n_{as}	D (nm)	Σ (Å^2)
s_1 pure	0	20.25	309
as/s_1 (25/75)	0.115	23.8	313
as/s_1 (50/50)	0.28	29.4	311
as/s_1 (54/46)	0.32	31.2	304
as/s_1 (59/41)	0.365	31.9	312

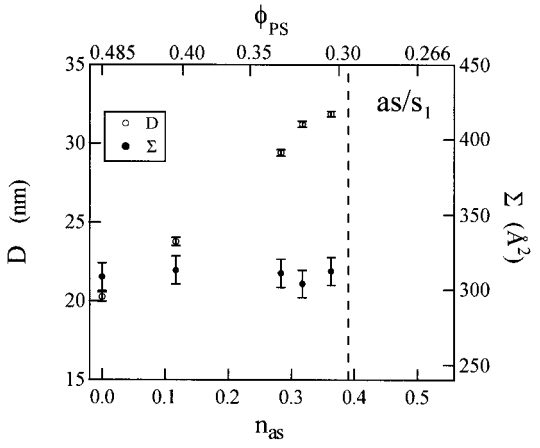

Figure 3. Blends *as*/s_1: lamellae thickness, D, and average interfacial area per junction, Σ, as a function of the fraction of *as* chains in the blend, n_{as}. The vertical dotted line indicates the stability limit of the lamellar morphology.

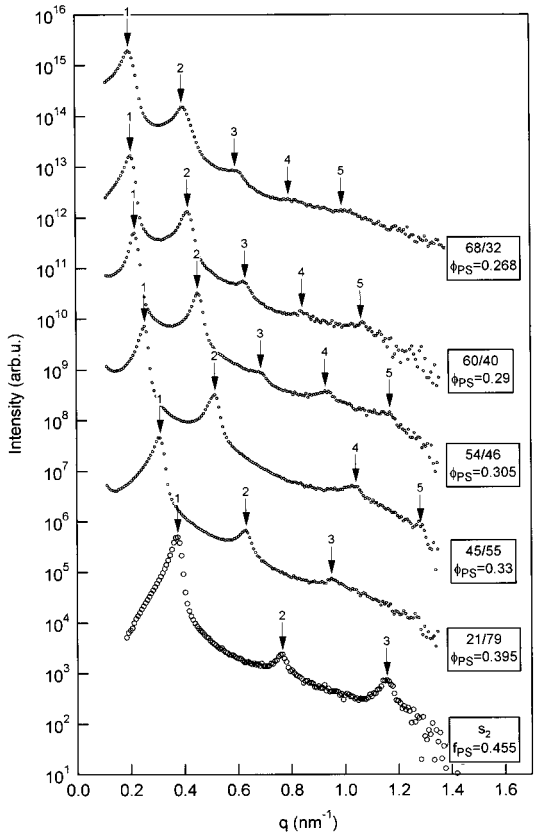

Figure 4. SAXS profiles from neat s_2 diblock and five blends as/s_2, 21/79, 45/55, 54/46, 60/40, and 68/32. The composition of the blends is expressed in weight percent of each diblock. Φ_{PS} has the same meaning as that in Figure 2.

Table 3. Characteristics of the Blends of the as/s_2 Series Presenting a Lamellar Morphology

blend	n_{as}	D (nm)	Σ (Å^2)
s_2 pure	0	17	287
as/s_2 (21/79)	0.07	20.4	280
as/s_2 (35/65)	0.14	23.2	281
as/s_2 (45/55)	0.20	25.9	278
as/s_2 (54/46)	0.265	28.8	277
as/s_2 (60/40)	0.31	30.5	279
as/s_2 (68/32)	0.39	32	294

s_1 or s_2 brushes should have the same conformation as that of s_1 or s_2.

III.3. as/s_3 Mixtures. The symmetric diblock s_3 is in a disordered state at room temperature. The behavior of the blends as/s_3 is therefore slightly more complex than that of the previous ones investigated. The SAXS profiles of several blends are presented in Figure 6. Below w_{as} of 0.39, the blends remain in a disordered state as shown in Figure 6. Upon further increase of the amount of the *as* chains, the blends exhibit a lamellar morphology. This morphology is stable up to w_{as} of 0.78. This blend (as/s_3 = 78/22) corresponds to the strongest shift of the stability limits for the lamellae we observed; it presents a lamellar morphology down to Φ_{PS} value as low as 0.245.

The period D determined experimentally and the interfacial area per junction Σ calculated for each system are summarized in Table 4. Figure 7 represents the values D and Σ as a function of the blend composition n_{as}.

In this system, as s_3 is in a disordered state, Σ_0 cannot be measured. Furthermore, it is very likely that blends with compositions close to the order−disorder transition

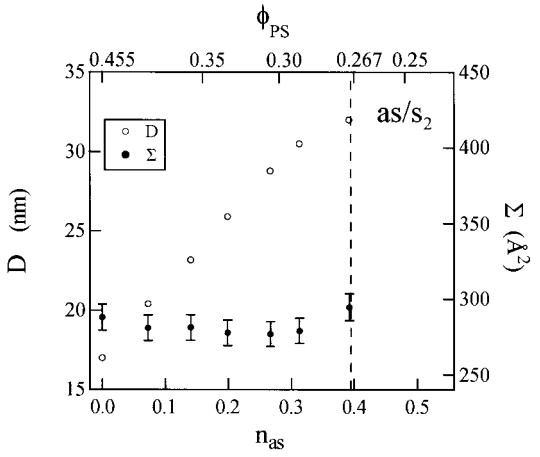

Figure 5. Blends as/s_2: lamellae thickness, D, and average interfacial area per junction, Σ, as a function of the fraction of *as* chains in the blend, n_{as}. The vertical dotted line indicates the stability limit of the lamellar morphology.

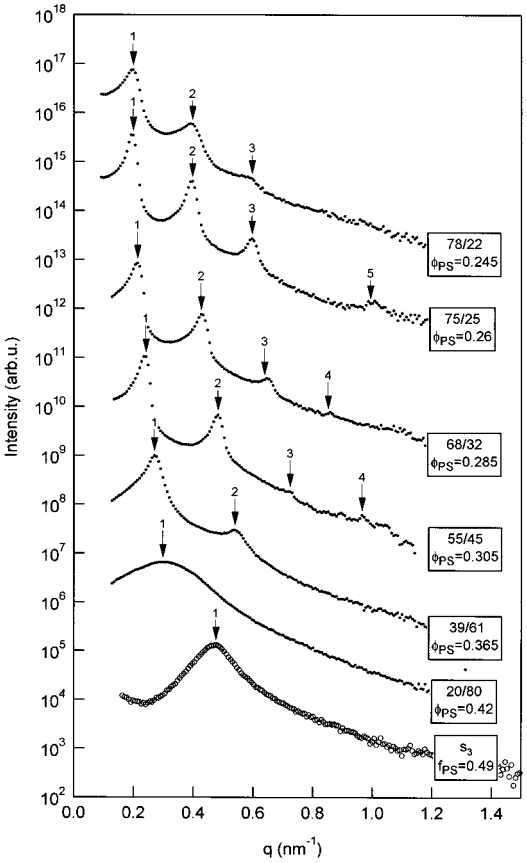

Figure 6. SAXS profiles from neat s_3 diblock and six blends of as/s_3, 20/80 to 78/22. Φ_{PS} has the same meaning as that in Figure 2.

(n_{as} = 0.12) are not in the strong segregation regime. In such a case, the assumption used to calculate Σ would not be valid. The fact that, unlike in the previous series, Σ is not strictly constant over the whole composition range could be a consequence of a breakdown of the assumption. Nevertheless, the same qualitative tendency as that for as/s_1 and as/s_2 is observed: Σ varies only by 10% with increasing n_{as} = 0.185 to n_{as} = 0.485, while D increases by 40%.

Before closing this section, it may be worth noting that the intensity of a particular higher order peak is suppressed compared with the intensities with other

Table 4. Characteristics of the Blends of the as/s_3 Series Presenting a Lamellar Morphology

blend	n_{as}	D (nm)	Σ (Å^2)
as/s_3 (39/61)	0.145	23.2	253
as/s_3 (45/55)	0.185	23.5	271
as/s_3 (55/45)	0.26	26.35	278
as/s_3 (68/32)	0.34	29.1	284
as/s_3 (71/29)	0.385	31.7	280
as/s_3 (75/25)	0.435	32.4	292
as/s_3 (78/22)	0.485	32.7	308

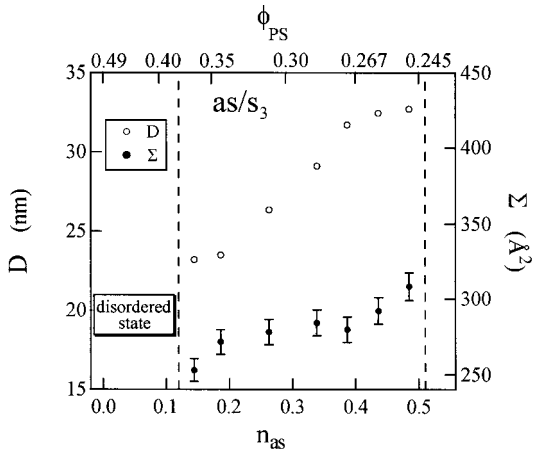

Figure 7. Blends as/s_3: lamellae thickness, D, and average interfacial area per junction, Σ, as a function of the fraction of as chains in the blend, n_{as}. The vertical dotted lines at $n_{as} \simeq 0.1$ and 0.5 indicate the lower and upper stability limits of the lamellar morphology, respectively.

higher order peaks in the SAXS profiles for the ordered lamellae, e.g., the third-order peak for the 50/50 blend of as/s_1 in Figure 2 and the 45/55 blend of as/s_2 in Figure 4 and the fourth-order peak for the 75/25 blend of as/s_3 in Figure 6. This is not an artifact but rather reflects the fact that the form factor $I_{form}(q)$ from one of the PS or PI lamellae goes to zero at the nth order peak position ($q = 2\pi n/D \equiv q_n$) of the one-dimensional lamellar array where $n = 3$ or 4 in this case. Since $I_{form}(q=q_n)$ is given by $I_{form}(q=q_n) \sim \sin^2(\pi n\Phi_{PS})/(\pi n\Phi_{PS})^2$, the volume fraction of the PS lamellae, Φ_{PS}, can be estimated from the order n of the higher order peak with the suppressed peak intensity using the relationship of $n\Phi_{PS} = 1$. Thus, $\Phi_{PS} = {}^1/_3$ or ${}^1/_4$ for the experimental situations mentioned above.

IV. Discussion

In the previous sections, we have shown experimentally that the chains organization in a lamellar structure of the binary mixtures of the diblocks was peculiar. Over the broad range of composition, when the mixture is rich in short symmetric diblocks, they seem to control the structure of the interface; i.e., the average interfacial area per junction in the blend is equal to the average interfacial area per junction in the pure short symmetric diblocks. In the present section we will present some theoretical models that could describe our experimental results. The interest of this work is that each model is based on different physical assumptions, i.e., different descriptions of the organization of the short and long diblocks in a common microdomain space with their junctions mixed on a common interface. The simplest model to be considered is that blend behaves as a pure diblock with its molecular weight being the same as that of number-average molecular weight of the blends

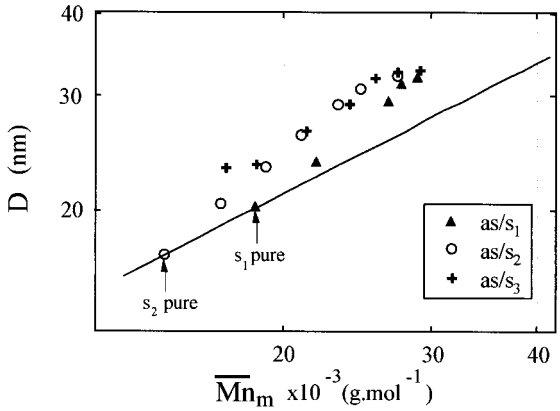

Figure 8. Plot of log D as a function of log $\bar{M}_{n,m}$. D is the lamellae thickness, and $\bar{M}_{n,m}$ is the number-average molecular weight of the mixture. The straight line corresponds to the equation $D = 0.029\bar{M}_{n,m}^{2/3}$.

(section IV.1).[19] The other models were developed especially for mixtures of chains (or diblocks) of different length, and here a theoretical prediction by the Birshtein, Zhulina, and Lyastkaya model (BZL model)[20,21] will be presented in section IV.2. Our experimental results and those of Hadziioannou and Skoulios will be compared with the BZL model[20,21] in sections IV.3 and IV.4, respectively. Finally, the other representative works[4,5] will be briefly presented in section IV.5.

IV.1. Uniform Mixing Model. The Helfand's model[22] in the context of the narrow interface approximation predicts that the lamellar thickness of a diblock copolymer is related to its degree of polymerization (or molecular weight) by the following power law.

$$D = k\bar{M}_n^{2/3} \tag{10}$$

Several authors have tested the accuracy of this model to describe experimental results obtained on pure diblocks[23] and on pure ABA triblocks[16] as well. In the latter case, the average molecular weight used in the equation is half the average molecular weight of the triblock. The former study concluded that the model and the experimental results are in close agreement.

To check whether this expression can describe the behavior of the blends of the diblock copolymers[19] investigated in the present study, one must introduce the average molecular weight of the mixture, $\bar{M}_{n,m}$, which is given by the following equation:

$$\bar{M}_{n,m} = (1 - n_{as})\bar{M}_{n,si} + n_{as}\bar{M}_{n,as} \tag{11}$$

The lamellae thickness, D, of the different blend samples investigated in the present study is represented in Figure 8 as a function log $\bar{M}_{n,m}$. Although the previous results reported by Hadzioannou and Skoulios[16] were reasonably predicted by eq 12,[19] the present results obtained for the blends having a large molecular weight and composition difference cannot be predicted by

$$D = k\bar{M}_{n,m}^{2/3} \tag{12}$$

On the other hand, the results obtained on the two pure diblocks, s_1 and s_2, are consistent with Helfand's model, the parameter k in eq 10 being chosen equal to 0.029 (Figure 8). From Figure 8, we can conclude that the lamellae composed of a binary mixtures of diblocks as/s_i are systematically thicker than the lamellae which

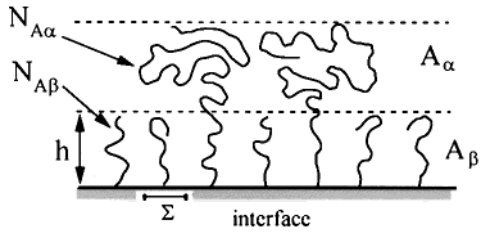

Figure 9. Structure of a mixed brush, with a grafting density at the interface $1/\Sigma$, comprised of a bipopulation of chains: $N_{A\beta}$ and $N_{A\alpha}$ are the degree of polymerization of the short and the long chains, respectively, and n_2 is the number fraction of long chains in the mixed brush. The A brush is composed of the A_β brush and A_α brush. In the BZL model the A_β brush is composed of both the short diblocks and subchains of the long diblocks with degree of polymerization $N_{A\beta}$, while the A_α brush is composed of only subchains of the long diblocks with degree of polymerization ($N_{A\alpha} - N_{A\beta}$) with a grafting density n_2/Σ on the plane parallel to and distance h apart from the interface.

would be composed of neat diblocks having the same number-average molecular weight as that of the mixtures.

IV.2. Birshtein, Zhulina, and Lyatskaya Model (BZL Model). IV.2.1. Description of the Model. Birshtein, Zhulina, and Lyastkaya have developed a model to describe the thermodynamics of polydisperse A−B diblocks in the strong segregation regime, i.e., when the junctions between blocks A and B are all located at the interface between A and B microdomains and A and B segregate themselves into their own domains. The surface tension, γ', is used to characterize the repulsion between A and B chemical species. As a simplification, monomers A and B are considered to have the same molecular volume, $v_m = a^3$, and the same Kuhn length, pa. The authors proposed a different expression of the free energy of the system for lamellar[21] and cylindrical[24−26] morphology. The authors consider the lamellar morphology as two polydisperse brushes grafted on each side of an interface (as schematically shown in Figure 9 for the A domain). The free energy of the system can then be described as the sum of the free energy of each brush, ΔF_A, ΔF_B (elastic energy), the surface free energy ΔF_{surf}, and the entropy of mixing, though, the last contribution can be neglected.[25] The expression of the free energy of the system then becomes

$$\Delta F = \Delta F_A + \Delta F_B + \Delta F_{surf} \tag{13}$$

The surface free energy represents the repulsion between the two chemically different brushes and is proportional to the average interfacial area per junction, Σ.

$$\Delta F_{surf} = \frac{\gamma\Sigma}{\bar{N}a^2} \tag{14}$$

where eq 14 represents the surface free energy per monomer, $\bar{N}$ is the average degree of polymerization of the block chains, and γ is the interfacial free energy per surface unit of a^2 ($\gamma = \gamma' a^2$), expressed in kT units.

The expression of the elastic energy of each brush A and B can be taken from the Milner and Witten[27] work on the free energy of a polydisperse brush grafted on a plane surface. (The key parameters are the chains distribution and the grafting density, σ.) Birshtein et al.[20] applied this model to calculate the elastic energy for a binary mixture of chains with different length, which is of prime interest for our study. They consider a mixture of short and long chains of degree of polymerization $N_{A\beta}$ and $N_{A\alpha}$, respectively (see Figure 9). The number fraction of long chains is n_2, and the grafting density at the interface $\sigma = 1/\Sigma$. A schematic representation of the mixed brush is shown in Figure 9. The authors make then a very important statement; they consider the mixed brush as the superposition of two monodisperse brushes, i.e., A_β and A_α brushes. The first brush (A_β) is composed of chains having DP of $N_{A\beta}$ with a grafting density $\sigma = 1/\Sigma$, and the second brush (A_α) (laying on top of the first one) is composed of chains of DP of $N_{A\alpha} - N_{A\beta}$ and a grafting density $\sigma = n_2/\Sigma$. The elastic energy of the brush A is then the sum of the elastic energies of the two monodisperse brushes. The elastic energy per chain of a monodisperse brush of chains of DP = N and grafting density $1/\Sigma$ is given by the following expression:

$$\Delta F_{el}(N,\Sigma) = \frac{\pi^2}{8p}\left(\frac{\Sigma}{a^2}\right)^{-2} N \tag{15}$$

Hence

$$\Delta F_A = \Delta F_{el}(N_{A\beta},\Sigma) + n_2 \Delta F_{el}(N_{A\alpha} - N_{A\beta},\Sigma/n_2) \tag{16}$$

IV.2.2. Expression of the Free Energy of Blends *as*/s_i Using the BZL Model. Most of the binary mixtures of SI diblocks investigated in this study, *as*/s_i, are strongly segregated, and therefore, the BZL model could be used. But, before using this model, the following two simplifications are necessary. The BZL model considers A and B to have the same Kuhn lengths and the same specific volumes. According to the literature,[28] the Kuhn lengths of isoprene and styrene are 7 and 6.5 Å, respectively. We will consider both equal to 6.7 Å. The monomer volume will also be considered equal for both species, and hence we will use an average value of $v_m = 0.139$ nm^3 ($a = 0.52$ nm). Over the composition range investigated, this assumption does not introduce more than a 5% error.

Using an average monomer volume, $v_m = a^3$, greatly simplifies the expression of Σ as a function of the blend's characteristics; eq 8 becomes

$$\Sigma = 2a^3\bar{N}/D \tag{17}$$

where $\bar{N} = n_{as}N_{as} + (1 - n_{as})N_{si}$, and N_{si} (i = 1, 2, or 3) and N_{as} are total DP' s of s_i (i = 1, 2, or 3) and *as*, respectively.

(a) Elastic Energy. The elastic free energy of the blends *as*/s_i is the sum of the elastic free energies of the PS and PI brushes ($\Delta F_{el} = \Delta F_{PS} + \Delta F_{PI}$). Each of this brush is constituted of a bipopulation of chains having different lengths ($N_{si,PI}$, $N_{as,PI}$ and $N_{si,PS}$, $N_{as,PS}$). Using the BZL model (eq 16), their elastic free energy becomes

$$\Delta F_j = \Delta F(N_{si,j},\Sigma) + n_{as}\Delta F(N_{as,j} - N_{si,j},\Sigma/n_{as}) \tag{18}$$

where j = PS or PI. Using eq 15 leads to the following expression:

$$\Delta F_j = \frac{\pi^2}{8p}\left(\frac{\Sigma}{a^2}\right)^{-2} N_{si,j} + n_{as}\frac{\pi^2}{8p}\left(\frac{\Sigma}{n_{as}a^2}\right)^{-2}(N_{as,j} - N_{si,j}) \tag{19}$$

In the systems we investigated here, the long block belongs to the same chain on both side of the interface ($N_{as,PI} > N_{si,PI}$ and $N_{as,PS} = N_{si,PS}$; see Table 1). This

simplifies the expression of the total elastic energy per chain of the mixtures:

$$(\Delta F_{el})_{chain} = \Delta F_{PS} + \Delta F_{PI} = \frac{\pi^2}{8p}\left(\frac{\Sigma}{a^2}\right)^{-2} N_{si}\left\{1 + n_{as}{}^3\left(\frac{N_{as}}{N_{si}} - 1\right)\right\} \quad (20)$$

The elastic energy per monomer, ΔF_{el}, is obtained by dividing the elastic energy per chain by $\bar{N}$; thus

$$\Delta F_{el} = \frac{\pi^2}{8p}\left(\frac{\Sigma}{a^2}\right)^{-2} f(n_{as}) \quad \text{with}$$

$$f(n_{as}) = \frac{1 + n_{as}{}^3\left(\frac{N_{as}}{N_{si}} - 1\right)}{1 + n_{as}\left(\frac{N_{as}}{N_{si}} - 1\right)} \quad (21)$$

(b) Total Free Energy. The expression of the total free energy per monomer is obtained through eqs 13, 14, and 21:

$$\Delta F = \frac{\gamma\Sigma}{\bar{N}a^2} + \frac{\pi^2}{8p}\left(\frac{\Sigma}{a^2}\right)^{-2} f(n_{as}) \quad (22)$$

The total free energy is a function of Σ, and minimizing the free energy ΔF with respect to Σ leads to the equilibrium interface structure:

$$\frac{\partial \Delta F}{\partial \Sigma} = 0 \quad (23)$$

The equilibrium interfacial area is given by

$$\frac{\Sigma}{a^2} = \left(\frac{\pi^2}{4\gamma p}\right)^{1/3} f(n_{as})^{1/3} \bar{N}^{1/3} \quad (24)$$

The equilibrium lamellar spacing $D_{\alpha\beta}$ can therefore be predicted from the BZL model, using eqs 17 and 24

$$D_{\alpha\beta} = 2a\left(\frac{4\gamma p}{\pi^2}\right)^{1/3} f(n_{as})^{-1/3} \bar{N}^{2/3} \quad (25)$$

while the lamellar spacing for pure short diblock copolymer, D_β, is easily obtained as $D_\beta = 2a(4\gamma p/\pi^2)^{1/3} N_\beta{}^{2/3}$ from eq 25, and the ratio of $D_{\alpha\beta}$ to D_β is given by

$$\frac{D_{\alpha\beta}}{D_\beta} = \left[1 + n_{as}\left(\frac{N_\alpha}{N_\beta} - 1\right)\right]\left[1 + n_{as}\left(\frac{N_\alpha}{N_\beta} - 1\right)\right]^{-1/3} \quad (26)$$

Equation 24 shows that the average interfacial area per junction of a blend containing n_{as} long diblocks depends on the (total) DP of the two diblocks (N_{as}, N_{si}) and on the characteristics of the chemical species (a, p, γ). The average monomer volume and the Kuhn length have been chosen on the basis of literature data on styrene and isoprene monomers. Therefore, the BZL model (eq 24) can be used to fit our experimental data with only one adjustable parameter, γ. The surface tension which characterizes the repulsion between the two chemical species can be linked to Flory's ineraction parameter χ_{SI}.[12,29] This parameter is independent of the block lengths. Therefore, in the theoretical equations, the only parameter that distinguishes the three series of the mixtures, as/s_1, as/s_2, and as/s_3, is the ratio $r \equiv N_{as}/N_{si}$, which has been used to represent the phase diagram of these mixtures. The $^2/_3$ power law with respect to $\bar{N}$ or $\bar{M}_{n,m}$ is unaltered, but the proportionality constant depends on the chain organization of the long and short diblocks in the microdomain space (cf. eqs 12 and 25).

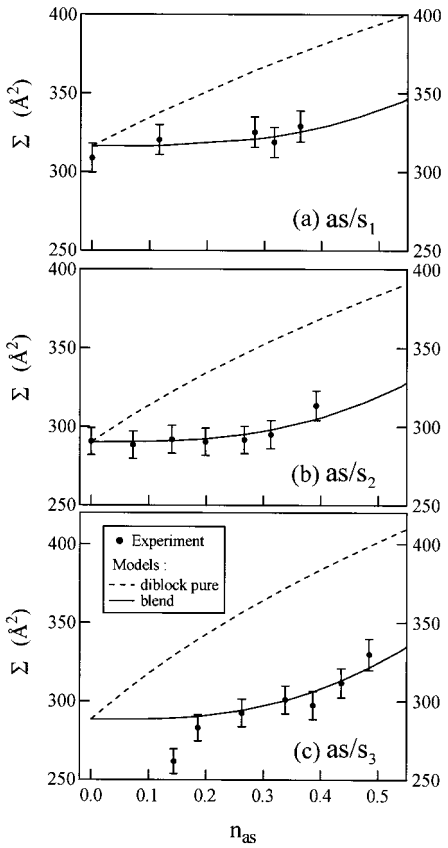

Figure 10. Mixtures as/s_1 (a), as/s_2 (b), and as/s_3 (c): average interfacial area per junction as a function of the number fraction n_{as} of long asymmetric diblock *as*, determined experimentally (points), calculated using the BZL model (solid line), and calculated for the equivalent pure diblock (dotted line).

IV.3. Comparison between Experimental and Theoretical Results. The changes of the interfacial area per junction, Σ, with n_{as} for the three series of blends investigated are represented in Figure 10. Together with the experimental results is plotted the curve obtained from BZL model using eq 24. The values of γ corresponding to the best fit are 0.269, 0.264, and 0.236 in parts a, b, and c of Figure 10, respectively. For the sake of comparison is plotted also the value Σ predicted for the pure diblock having an average degree of polymerization equal to that of the blend (broken line).

For the three systems investigated, the agreement between the experimental results and the BZL model is very satisfactory; the tendency is clearly predicted by the model. Adding long asymmetric diblocks to short symmetric ones does not modify significantly the interfacial area per junction. The structure of the interface is essentially controlled by the short chains. Furthermore, the only adjustable parameter used to fit the experimental data, γ, is found to be roughly the same for the three series of blends investigated, $\gamma \approx 0.26$. The interfacial free energy per surface area of a^2 in units of kT, γ, allows us to determine the interfacial tension between PS and PI.

$$\gamma' = (\gamma/a^2)kT \tag{27}$$

which leads to $\gamma' = 4.6 \times 10^{-3}$ N m^{-1} with $a = 0.518$ nm, $k = 1.38 \times 10^{-23}$ J K^{-1}, $T = 303$ K, and $\gamma = 0.26$.

The interfacial tension between PS and PI can be computed using Wu's equation[30] (eq 28) and data from the literature (Table 5) concerning the surface tension of each component:

$$\gamma_{12} = \gamma_1 + \gamma_2 - \frac{4\gamma_1^d\gamma_2^d}{\gamma_1^d + \gamma_2^d} - \frac{4\gamma_1^p\gamma_2^p}{\gamma_1^p + \gamma_2^p} \tag{28}$$

where γ_{12} represents the interfacial tension between polymer 1 and 2, and γ_i ($i = 1$ or 2) denotes the surface tension of the ith polymer which can be separated into dispersion (nonpolar) and polar components, i.e., $\gamma_i = \gamma_i^d + \gamma_i^p$. Here, γ_i^d and γ_i^p represent the surface tension of the ith polymer arising from dispersion force interactions (d) and various dipolar and specific interactions (p), respectively. The value obtained is

$$\gamma'_{SI} = (3.3 \pm 0.2) \times 10^{-3} \text{ N m}^{-1}$$

This value and the value extracted from the best fitting of our experimental results with BZL model are of the same order of magnitude. Therefore, we can conclude that BZL model gives a quantitative description of our results.

The experimental results on $D_{\alpha\beta}/D_\beta$ for the series of as/s_1, as/s_2, and as/s_3 are further compared with the predictions obtained with the different models in parts a, b, and c of Figure 11, respectively. The BZL model again gives a good description of our experimental results. The stability range of the lamellar morphology, as shown with a composition range given by arrow(s), has been significantly enlarged due to the cosurfactant effect.[1] (The effects of blended diblocks differing in lengths and compositions share a common interface.)

IV.4. Comparison with the Hadziioannou and Skoulios Experimental Results. Hadziioannou and Skoulios investigated the binary blends of SI diblocks having both lamellar morphology but differing in molecular weight with r being 2.7.[2] The characteristics of their SI blocks are summarized in Table 6. Using small-angle scattering, they determined the lamellar spacing, $D_{\alpha\beta}$, of the blends SI-3/SI-5 with different compositions. We represented their experimental results in Figure 12, together with the curves predicted by BZL model, and a pure diblock having an average degree of polymerization equal to that of the blend, respectively.

The agreement is not perfect between experimental data and the predicted curves, but it can be clearly observed that the lamellar spacing predicted by the uniform mixing model (the pure diblocks) never gets thicker than the lamellae of the blends. The experimental data are located between the theoretical curves of the BZL model and the pure diblock having average molecular weight of the blend. We cannot decide which model fits better to the experiment for the SI-3/SI-5 blends.

IV.5. Remarks about the Other Theoretical Works. We have concluded that the BZL model can describe our results, though it might not be the only model. Spontak also proposed a model to predict the lamellae thickness of binary mixtures of diblocks.[4]

As in the BZL model, Spontak considers the lamellae as two brushes grafted on each side of a plane surface.

Table 5. Surface Tensions of Polystyrene and Polyisoprene[28,31]

polymer	γ_i (10^{-3} N m^{-1})	γ_i^d (10^{-3} N m^{-1})	γ_i^p (10^{-3} N m^{-1})
polystyrene	40, 7	33, 7	7
polyisoprene	31−32	29.2−30.1	1.8−1.9

Table 6. Characteristics of the SI Diblocks Investigated by Hadziioannou and Skoulios[2]

diblock	$\bar{M}_n \times 10^{-3}$	f_{PS}	morphology
SI-3	27	0.5	lamellar
SI-5	72	0.5	lamellar

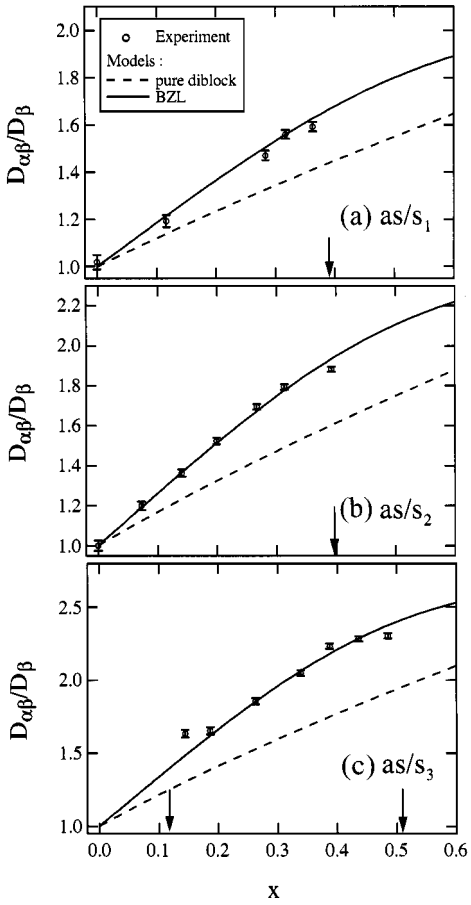

Figure 11. Mixtures as/s_1 (a), as/s_2 (b), and as/s_3 (c): comparison between the experimental results and the two theoretical predictions. The arrow indicates the lower and upper stability limits of the lamellar morphology.

However, the major difference lies in the mixed brush organization (Figure 9). Birshtein et al. consider that the number of monomers of the long chain that participate in the brush layer composed of the short block A_β anchored at the interface, $\Gamma N_{A\alpha}$ (brush A_β in Figure 9), is equal to the degree of polymerization of the short diblock, $N_{A\beta}$, hence $\Gamma = N_{A\beta}/N_{A\alpha}$,[20] whereas in ref 4, Spontak considers Γ as an adjustable parameter, which depends on the blending composition. The stable structure of the mixed brush is then found by minimizing the free energy of the system with respect to Γ. The minimization of the free energy with respect to Γ leads to Γ^*, which corresponds to the thermodynamically stable organization of the mixed lamellae. $\Gamma^*/(N_\beta/N_\alpha)$ numerically evaluated as a function of n_{as} monotonically decreases from unity to zero with increasing n_{as} from 0 to 1 (cf. eq 26 or Figure 3 of ref 4), whereas it is unity, independent of n_{as}, in the assumption of BZL. Furthermore, in ref 4, Spontak gave the expression for $D_{\alpha\beta}/D_\alpha$

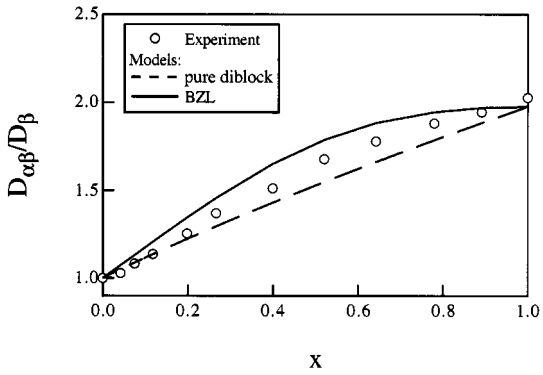

Figure 12. Mixtures SI-3/SI-5: comparison between experimental results (from Hadziioannou et al.) and theoretical predictions. In these blends the morphologies are lamella at any blend compositions.

(D_α is the lamellar spacing of the pure long diblock), corresponding to $D_{\alpha\beta}/D_\beta$ in eq 25. The Spontak model gave a satisfactory agreement with the experimental results on $D_{\alpha\beta}/D_\beta$, though the BZL model gave a better prediction than the Spontak model. Later on, Matsen[32] pointed out that the Spontak's model[4] incorrectly evaluated Γ (or Γ^*). Spontak had accepted this suggestion, and in his later work[5] he and co-workers analyzed their data with their modified version[5] which resulted in a better agreement between the experimental and theoretical results. However, we note that the modified version did lead their model to be identical to the BZL model. The numerical results for $D_{\alpha\beta}/D_\beta$ on our as/s_i systems calculated on the basis of the modified version[5] were naturally identical to those predicted with the BZL model.

Matsen proposed a highly advanced self-consistent-field theory (SCFT) which can apply not only to the strong segregation regime but also to the intermediate regime.[32] However, at the same time, he suggested that the BZL model can give rather good approximation to SCFT with respect to the lamellar spacing of the blend $D_{\alpha\beta}$ (cf. Figure 3 of ref 32).

V. Conclusion

The BZL model is in close agreement with our experimental results on binary mixtures of SI diblocks having different lengths and morphologies. However, the prediction of the model is less satisfactory on the experimental results for the mixtures of SI diblocks having a smaller molecular weight difference ($r = 2.7$)[2] in comparison to that on the above case of $r = 2.9$, 3.6, and 4.4. The less satisfactory agreement between the theoretical and experimental results for the mixture with $r = 2.7$ may be well expected from the assumption introduced into the model. The fit of our experimental results is achieved with only one adjustable parameter. This parameter represents the repulsion between the two chemical species styrene and isoprene. Therefore, in the three binary mixtures investigated, the best fit should be obtained with the same value for the adjustable parameter, and this is the case. The value obtained is in close agreement with the interfacial tension between those two polymers computed by other means.

These results validate (or strengthen) the description of the chains organization within a mixed brush given by Birshtein, Zhulina, and Lyastkaya.[20,21] A brush grafted on a surface constituted of a bipopulation of long and short chains is not equivalent to a brush of monodisperse chains having the average degree of polymerization of the blend. On the contrary, it should be viewed as two monodisperse brushes lying on top of each other. The first brush is constituted of the short chains with DP equal to N_s and the N_s monomers of the first subchains in the long chains. While the second brush is constituted of the extra length of the long chains and has a reduced grafting density, n_{as}/Σ, where n_{as} is the fraction of long chains in the mixture and $1/\Sigma$ is the grafting density of the mixed brush on the interface.

Furthermore, concerning the series of binary mixtures investigated in this study, as/s_i ($i = 1$, 2, or 3), the BZL model shows that the change of the domain spacing (lamellae thickness) with the blend's composition is controlled by the ratio between the lengths of the two diblocks, N_{as}/N_s. Over the composition range that was experimentally investigated on the mixtures as/s_i ($i = 1$, 2, or 3), it can be approximated that the addition of the long diblocks does not modify the organization of the interface. The short diblocks control the average interfacial arera per junction to the blend, $\Sigma = \Sigma_0$. As a consequence, the following important points are reduced: (i) for a given $r = N_{as}/N_{si}$, the larger the fraction of the long asymmetric blocks n_{as}, the larger the domain size; (ii) for a given blend composition n_{as}, the larger the value r, the larger the domain size. These features reduced from our experimental analysis are also predicted by the BZL theory.

The model that has been validated on binary mixtures could be extended to polydisperse chains distributions. It can be predicted that two samples having the same average degree of polymerization, one constituted of a monodisperse distribution of diblocks and the other constituted of a polydisperse distribution of diblocks, will not have the same domain spacing. The lamellae of the polydisperse sample will be thicker than the ones of the monodisperse sample.

References and Notes

(1) Court, F.; Hashimoto, T. *Macromolecules* **2001**, *34*, 2536 and references therein.
(2) Hadziioannou, G.; Skoulios, A. *Macromolecules* **1982**, *15*, 267.
(3) Vilesov, A. D.; Floudas, G.; Pakula, T.; Melenevskaya, E. Y.; Birshtein, T. M.; Lyatskaya, Y. V. *Macromol. Chem. Phys.* **1994**, *195*, 2317.
(4) Spontak, R. J. *Macromolecules* **1994**, *27*, 6363.
(5) Kane, L.; Satkowski, M. M.; Smith, S. D.; Spontak, R. J. *Macromolecules* **1996**, *29*, 8862.
(6) Lin, E. K.; Gast, A. P.; Shi, A.-C.; Noolandi, J.; Smith, S. D. *Macromolecules* **1996**, *29*, 5920.
(7) Fujimura, M.; Hashimoto, T.; Kawai, H. *Mem. Fac. Eng., Kyoto Univ.* **1981**, *43* (2), 224.
(8) Hashimoto, T.; Suehiro, S.; Shibayama, M.; Saijo, K.; Kawai, H. *Polym. J.* **1981**, *13*, 501.
(9) Suehiro, S.; Saijo, K.; Ohta, Y.; Hashimoto, T. *Anal. Chim. Acta* **1986**, *189*, 41.
(10) Balta-Calleja, F. J.; Vonk, C. G. *X-ray Scattering of Synthetic Polymers*; Elsevier: Amsterdam, 1989.
(11) Hendricks, R. W. *J. Appl. Crystallogr.* **1972**, *5*, 315.
(12) Helfand, E.; Tagami, Y. *J. Polym. Sci., Polym. Lett. Ed.* **1971**, *9*, 741. *J. Chem. Phys.* **1972**, *56*, 3592. *J. Chem. Phys.* **1972**, *57*, 1812.
(13) Helfand, E. *Polym. Prepr. (Am. Chem. Soc., Div. Polym. Chem.)* **1974**, *15*, 246. *J. Chem. Phys.* **1975**, *62*, 999. *Macromolecules* **1975**, *8*, 552.
(14) Helfand, E.; Wasserman, Z. R. *Macromolecules* **1976**, *9*, 879. *Polym. Eng. Sci.* **1977**, *17*, 582.
(15) Helfand, E.; Sapse, A. M. *J. Chem. Phys.* **1975**, *62*, 1327.
(16) Hadziioannou, G.; Skoulios, A. *Macromolecules* **1982**, *15*, 258.
(17) Ni, S.; Sakamoto, N.; Hashimoto, T.; Winnik, M. A. *Macromolecules* **1995**, *28*, 8686.

(18) Matsushita, Y.; Mori, K.; Mogi, Y.; Saguchi, R.; Noda, I.; Nagasawa, M.; Chang, T.; Glinka, C. J.; Han, C. C. *Macromolecules* **1990**, *23*, 4317.
(19) Hashimoto, T. *Macromolecules* **1982**, *15*, 1548.
(20) Birshtein, T. M.; Liatskaya, Y. V.; Zhulina, E. B. *Polymer* **1990**, *31*, 2185.
(21) Zhulina, E. B.; Birshtein, T. M. *Polymer* **1991**, *32*, 1299.
(22) Helfand, E.; Wasserman, Z. R. In *Developments in Block Copolymers-1*; Goodman, I., Ed.; Applied Science: Oxford, 1982.
(23) Hashimoto, T.; Shibayama, M.; Kawai, H. *Macromolecules* **1980**, *13*, 1237. Hashimoto, T.; Fujimura, M.; Kawai, H. *Macromolecules* **1980**, *13*, 1660.
(24) Zhulina, E. B.; Lyatskaya, Y. V.; Birshtein, T. M. *Polymer* **1992**, *33*, 332.
(25) Lyatskaya, J. V.; Zhulina, E. B.; Birshtein, T. M. *Polymer* **1992**, *33*, 343.
(26) Birshtein, T. M.; Lyatskaya, Y. V.; Zhulina, E. B. *Polymer* **1992**, *33*, 2750.
(27) Milner, S. T.; Witten, T. A. *J. Phys. (Paris)* **1988**, *49*, 1951.
(28) Brandrup, J.; Immergut, E. H. *Polymer Handbook*; John Wiley and Sons: New York, 1989.
(29) Leibler, L. *Makromol. Chem. Macromol. Symp.* **1988**, *16*, 1.
(30) Wu, S. *Polymer Interface and Adhesion*; Marcel Dekker: New York, 1982.
(31) Olabisi, O.; Robeson, L. M.; Shaw, M. T. *Polymer−Polymer Miscibility*; Academic Press: New York, 1979
(32) Matsen, M. W. *J. Chem. Phys.* **1995**, *103*, 3268.

MA011588C